Journal of Molecular Graphics and Modelling 61 (2015) 224–230

Contents lists available at ScienceDirect

Journal of Molecular Graphics and Modelling

journal homepage: www.elsevier.com/locate/JMGM

Band structure of graphene modulated by Ti or N dopants and applications in gas sensoring

Hong-ping Zhang[a,b,*], Xue-gang Luo[a], Xiao-yan Lin[a], Ya-ping Zhang[a], Ping-ping Tang[a], Xiong Lu[c], Youhong Tang[d,**]

[a] Engineering Research Center of Biomass Materials, Ministry of Education, School of Materials Science and Engineering, Southwest University of Science and Technology, Mianyang, Sichuan 621010, China
[b] Western Mining Co. Ltd, The Key Laboratory of Mineral Processing and Comprehensive Utilization in the Plateau of Qinghai Province, Xining, Qinhai 810007, China
[c] Key Laboratory of Advanced Technologies of Materials, Ministry of Education, School of Materials Science and Engineering, Southwest Jiaotong University, Chengdu, Sichuan 610031, China
[d] Centre for NanoScale Science and Technology and School of Computer Science, Engineering and Mathematics, Flinders University, South Australia 5042, Australia

ARTICLE INFO

Article history:
Received 15 March 2015
Received in revised form 18 July 2015
Accepted 5 August 2015
Available online 8 August 2015

Keywords:
HOMO–LUMO gap
Nitrogen dioxide (NO_2)
Graphene
Doping
Density functional theory

ABSTRACT

The exploration of novel sensors for NO_2 detection is particularly important in material and environmental sciences. In this work, the HOMO–LUMO gap of graphene, Ti- or N-doped graphene is investigated by DFT methods. The adsorption of NO_2, NO, and O_2 on Ti- or N-doped graphene of different sizes is also explored. Results reveal that the interactions between gases (NO_2, NO, and O_2) and Ti- or N-doped graphenes is not affected by the size of graphene. The doped Ti greatly improves the interactions between gases and graphene whereas the doped N has no effect on those interactions. The HOMO– LUMO gap of Ti-doped graphene can be modulated by adsorption of the gases. The cross effect of the NO and O_2 is also investigated, and it is demonstrated that Ti-doped graphene has specific interactions with NO_2. Thus, Ti-doped graphene can be a candidate for NO_2 sensor materials. Furthermore, doping the graphene with Ti or N improves the sensitivity of the sheets toward NO_2, which can be trapped and detected by the intrinsic graphene. Efficient sensors are rationally designed to diversify their applications in environmental science and engineering.

1. Introduction

Graphene has attracted considerable interest for its many specific properties and wide applications. It is a two-dimensional (2-D) material that is chemically inert. Its many excellent characteristics include good electronic properties, high levels of stiffness and strength, and thermal conductivity. The 2-D crystal structure of graphene causes electrons to behave like massless fermions, with the speed of light being replaced by a Fermi velocity of approximately 10^6 m/s. The electrons in graphene show high charge-carrier mobility [1–4]. Owing to its excellent properties, graphene is regarded as a promising functional material in many applications, for example, as nanofiller of composites, ultra-high frequency transistors, gas sensors, and potential electrode materials. Among relevant investigations, the potential of graphene as a gas sensor or sorbent has been extensively studied [5–6]. Meanwhile, doped graphene has attracted a great deal of research attention. Apart from N-doped graphene, other doped graphenes that have been extensively studied by computer simulation methods include transition metal-doped graphene (Ti-, Fe-, Al-, Pt- and so on) and B-doped graphene [7–9]. For N-doped graphene, both experimental and theoretical studies have been extensively performed.

Rojas and Leiva et al. [10] studied the interactions between small molecules and Ti-doped graphene sheet using density functional theory (DFT) calculations, and found that the Ti-doped graphene sheet could adsorb H_2 molecules. Similar results were obtained by Chu et al. [11]. Our previous studies demonstrated that Ti-doped graphene could greatly improve the interactions between small gas molecules and graphene [12]. Al-doped graphene sheet was found

* Corresponding author at: Engineering Research Center of Biomass Materials, Ministry of Education, School of Materials Science and Engineering, Southwest University of Science and Technology, Mianyang, Sichuan 621010, China. Fax: +86 816 6089009.
** Corresponding author. Fax: +61 8 82013618.
E-mail addresses: zhp1006@126.com (H.-p. Zhang), youhong.tang@flinders.edu.au (Y. Tang).

http://dx.doi.org/10.1016/j.jmgm.2015.08.004
1093-3263/

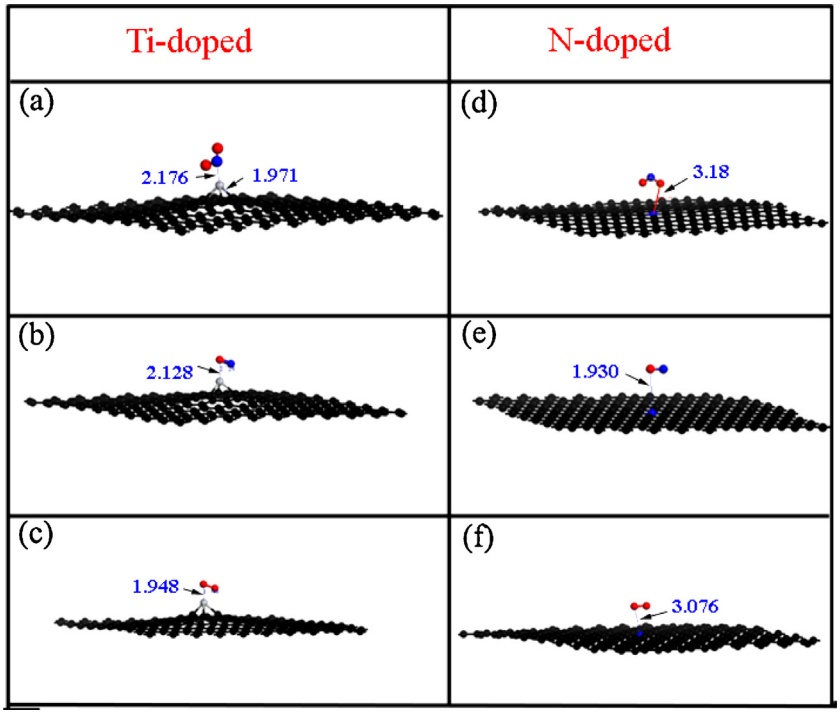

Fig. 1. Equilibrium configuration of Ti-doped graphene sheets and the corresponding HOMO–LUMO gap.

Table 1
Adsorption energies between gases (NO_2, NO and O_2) and Ti- or N-doped graphenes of different sizes (Unit: eV).

	200 atoms total		162 atoms total		98 atoms total		72 atoms total		32 atoms total	
	Ti-doped	N-doped	Ti-doped	N-doped	Ti-doped	N-doped	Ti-doped	N-doped	Ti-doped	N-doped
NO_2	−2.98	−0.44	−2.96	−0.44	−3.69	0.49	−2.91	−0.48	−3.03	−0.52
NO	−1.44	0.16	−1.37	0.14	−0.62	0.14	−1.4	0.14	−1.47	−0.08
O_2	−3.45	0.42	−3.32	0.38	−2.55	0.38	−3.3	0.38	−3.36	−0.19

to be a potential material for detecting formaldehyde. Ao et al. used DFT calculations to investigate the ideal H_2 storage distance of Al-doped graphene [13]. Experimental and theoretical studies have shown that N-doped graphene displays good activity as an electrocatalyst of oxygen reduction under certain conditions [14–16]. Anota et al [17] studied the interaction between the graphene sheet and the chitosan monomer by DFT methods and the biosorption processes of glucose and cholesterol on chitosan functionalized graphene have also been investigated. The interactions between small molecules and doped graphene have been studied by DFT calculations, and many doped graphenes have been found to display sensoring properties for small gas molecules. However, still lacking are detailed studies of the effect of doping density on the electronic structures of the graphene, and also potential applications in specific gas sensoring have not been reported.

Nitrogen dioxide (NO_2) is a common by-product in industrial synthesis, automotive engines, and power sources. It is a strong oxidizing agent that has C_{2v} point group symmetry. This highly toxic gas is considered a major air pollutant. Thus, various types of NO_2 sensors have been developed by researchers. Transition metals, including Pt, Pd, and Fe can be used as adsorption and decomposition media of NO_2 into NO and O_2 [18–21]. Pearce et al. [22] reported that graphene could be a sensor for NO_2 in a certain concentration range. Generally, the detection of NO_2 would be interrupted by other related gases such NO, O_2, and CO.

In this study, Ti- and N-doped graphene were systematically investigated and the effects of different doping densities on the electronic structures of graphenes were explored. The interactions between NO_2 and Ti- or N-doped graphene were studied. To determine whether the adsorption of NO and O_2 on Ti- or N-doped graphene would disturb the sensoring of NO_2, the interactions between Ti- or N-doped graphene and the other gas molecules (NO or O_2) were also investigated.

2. Computational details

Use of DFT methods can reveal important chemical and electron structure information about Ti- or N-doped graphene and NO_2-graphene adsorbed systems. Dmol^3 (Accelrys, San Diego, CA) is a highly accurate DFT program used to predict the equilibrium geometries of intrinsic or X-doped graphene, where X = Ti or N. Fundamental chemical information about NO_2-intrinsic or X-doped graphene adsorbed systems has been carefully studied. In simulations, physical wave functions were expanded in terms of numerical basis sets. A double numerical plus polarization (DNP) double numerical basis set [23] was used, which was comparable to the 6–31G** basis set [24–27]. Core electrons were treated with a DFT semi-core pseudopotential method. The exchange-correlation energy was calculated using Perdew–Burke–Ernzerhof (PBE) generalized gradient approximation (GGA) [28]. It was well known that GGA usually gives lower energy gaps than real experimental values, especially for semiconductors [29]. Considering that GGA should give the correct trends for the similar study systems (Ti or N doped graphene with various size) and the limitation of computational cost, GGA was chosen. The Sampling integration of special points over the Brillouin zone was employed by Monkhorst-Pack schemes with a $3 \times 3 \times 1$ k-point mesh [30]. A Fermi smearing of 0.005 Ha (1 Ha = 27.211 eV) and a global orbital cutoff of 5.2 Å were employed.

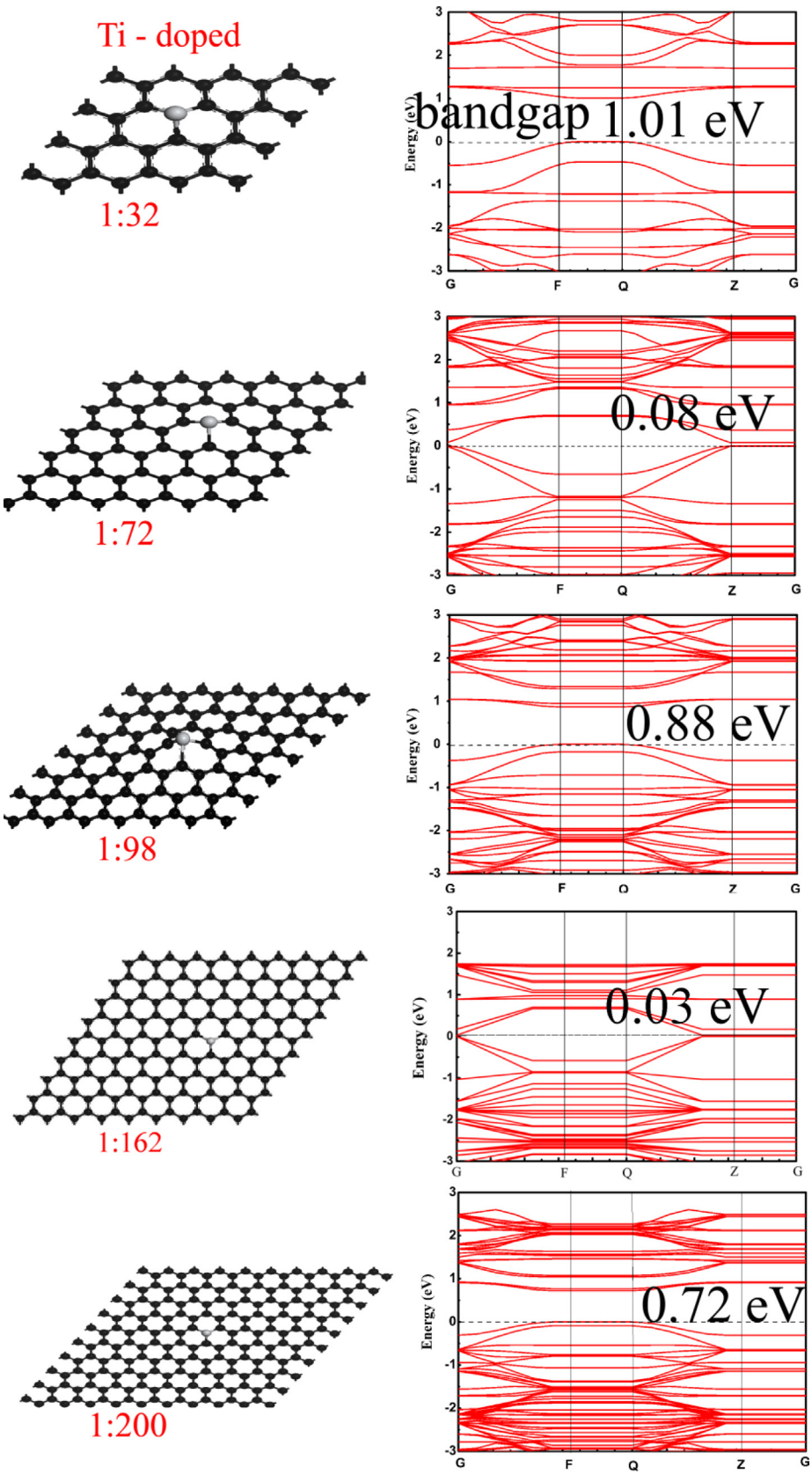

Fig. 2. Equilibrium configuration of N-doped graphene sheets and the corresponding HOMO–LUMO gap.

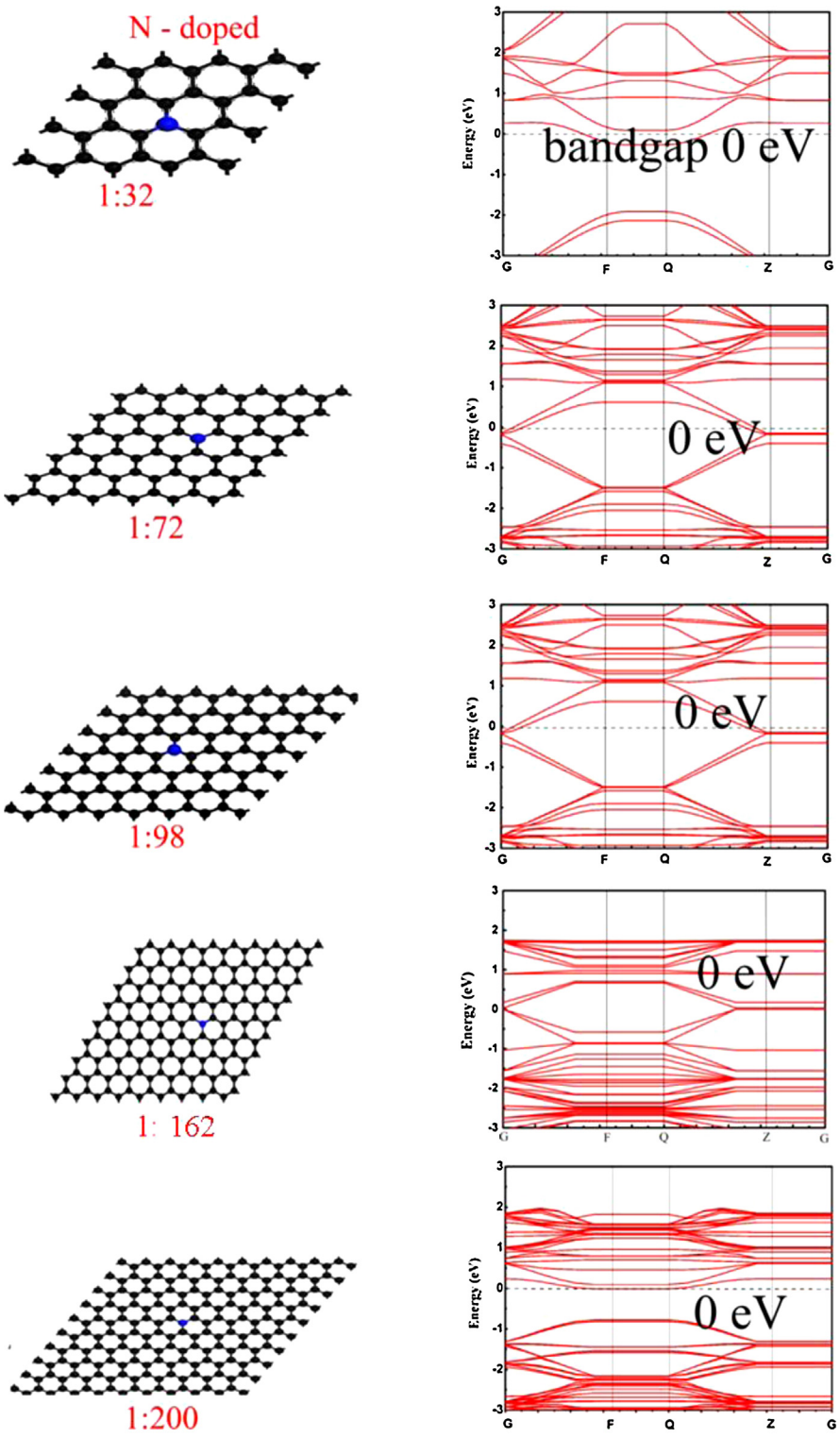

Fig. 3. Equilibrium configuration of Ti- or N-doped graphene sheets (200 atoms in total) with gases (NO_2, NO and O_2) adsorption on them.

Models of Ti- and N-doped graphene sheets were built by replacing one of the carbon atoms of graphene with a Ti or N atom. Then the Ab initial geometry optimization process was utilized to obtain Ti- or N-doped graphene with minimal energy. To investigate the different doping densities, three kinds of doped graphene model were built, with different ratios of the doping atoms and carbon atoms (1:32; 1:72; 1:98, 1:200).

The adsorption energy (E_{ads}) of NO_2, which indicates the intensity of interaction between an NO_2 molecule and a graphene sheet, is derived from Eq. (1):

$$E_{ads} = E_{(NO_2+graphene)} - (E_{NO_2} + E_{graphene}) \quad (1)$$

where $E_{NO_2+graphene}$, E_{NO_2}, and $E_{graphene}$ represent the total energy of a NO_2-graphene system, the energy of an NO_2 molecule, and the

energy of an intrinsic, Ti- or N-doped graphene sheet, respectively. E_{ads}< 0 corresponds to an exothermic adsorption process, and an increasingly negative E_{ads} indicates a highly stable adsorption. However, very strong interactions between gas and substrate materials do not imply an enhanced signal for good sensors. Removing gases from the substrate is very difficult. Conventional transition state theory states that:

$$\tau = \nu_0^{-1} \exp(\frac{-E_{ad}}{kT}) \quad (2)$$

where$\tau$is the recovery time, υ_0 is the attempt frequency, T is the temperature, and k is the Boltzmann's constant. A highly negative E_{ads} suggests a long recovery time. Hence, the interaction energy between NO_2 and doped graphene is directly related to the recovery time. Energy gaps (E_g) (the energy gap between the valence band and the conduction band) in different doped graphene systems were compared to analyze the response of NO_2 adsorption. Thus, E_g is an important factor for determining the electrical conductivity of the materials and is given as follows:

$$\sigma \propto \exp(\frac{-E_g}{2kT}) \quad (3)$$

where σ is the electrical conductivity of the material. A smaller E_g indicates higher conductance of the material at a specific temperature.

3. Results and discussion

3.1. HOMO–LUMO gap modulation by the doping density

Fig. 1 shows DFT optimized Ti- and N-doped graphene with adsorption of gas molecules (NO_2, NO and O_2). The HOMO–LUMO gap relates directly to the physical properties of the graphene. In this study, the HOMO–LUMO gap for pure, Ti- and N-doped graphene with different doping densities was calculated to investigate the effect of the two different dopants and the doping density on the HOMO–LUMO gap of graphene. Fig. 2 shows the optimized geometries of the Ti-doped graphene with different Ti doping densities and their HOMO–LUMO gap values. It can be observed that the HOMO–LUMO gap of the graphene could be adjusted by the doped Ti atom. When the atom ratio of Ti to C is 1:32, the HOMO–LUMO gap is 1.01 eV, which was very close to the silicon (about 1.1 eV). This result implies that this kind of graphene might possess semiconductor-like properties. When the atom ratio is 1:72, the HOMO–LUMO gap is 0.08 eV, which is very different from 1:32. However, when the atom ratio decreases to 1:98 and 1:200, the HOMO–LUMO gaps are 0.88 eV and 0.72 eV respectively. These results have not been previously reported. They indicate that the HOMO–LUMO gap of graphene can be modulated by the doping density of the Ti. It was already known widely that the conductivity of graphene could not be turned off, because it lacks a HOMO–LUMO gap in its electronic spectrum [31]. The HOMO–LUMO gap calculation of Ti-doped graphene indicates that Ti doping might be a promising way to open the graphene's HOMO–LUMO gap. For *N* doped graphene, the HOMO–LUMO gap was 0 eV for the four N doping densities (see Fig. 3). To explore the effect of Ti doping density on the HOMO–LUMO gap of graphene, we calculated the HOMO–LUMO gap of the various Ti-doped systems with different Ti densities, i.e., 1:18; 1:32; 1:40; 1:50; 1:60; 1:72; 1:84; 1:98; 1:128; 1:162, and 1:200. Fig. 4 shows the relationship between Ti-doped density and the HOMO–LUMO gap of the Ti-doped graphene. Table 5 shows the charge on the gas-doped graphene (1:72) systems. It indicated that the charges trends to transfer from doped graphene to the adsorbed gas molecules. Chernozatonskii et al. [32] reported that the effect of the different types of functionalization on the HOMO–LUMO gap of the graphene was related to the distance between the different defect regions. Our results confirm that altering the density of the doped Ti could be used to tune the HOMO–LUMO gap of graphene.

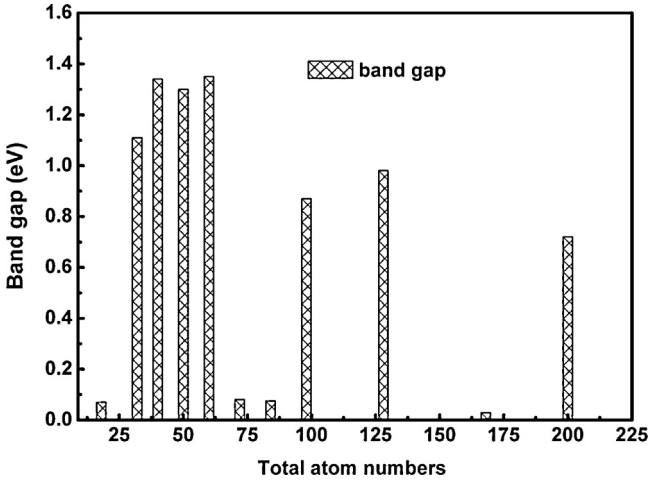

Fig. 4. Relationship between HOMO–LUMO gap values of Ti-doped graphene and total atom number (corresponding to the density of the Ti-doping, from 1:18 to 1:200).

3.2. NO_2 adsorption on Ti- or N-doped graphene

NO_2 adsorption on Ti- or N-doped graphene with four different sizes was studied by DFT calculation. Table 1 shows the adsorption

Table 2
Comparison of HOMO–LUMO gaps of Ti- or N-doped graphene before and after NO_2 adsorption.

	Pure	After adsorption		Pure	After adsorption
Ti (200)	0.72	0	N (200)	0	0.31
Ti (162)	0.03	0	N (162)	0	0
Ti (98)	0.87	0.91	N (98)	0	0.24
Ti (72)	0.08	0	N (72)	0	0
Ti (32)	1.01	0	N (32)	0	0.15

Table 3
Comparison of HOMO–LUMO gaps of Ti- or N-doped graphene before and after NO adsorption.

	Pure	After adsorption		Pure	After adsorption
Ti (200)	0.72	0	N (200)	0	0
Ti (162)	0.03	0	N (162)	0	0
Ti (98)	0.87	0.32	N (98)	0	0
Ti (72)	0.08	0	N (72)	0	0
Ti (32)	1.01	0	N (32)	0	0

Table 4
Comparison of HOMO–LUMO gaps of Ti- or N-doped graphenes before and after O_2 adsorption.

	Pure	After adsorption		Pure	After adsorption
Ti (200)	0.72	0.14	N (200)	0	0.17
Ti (162)	0.03	0	N (162)	0	0
Ti (98)	0.87	0.12	N (98)	0	0.11
Ti (72)	0.08	0	N (72)	0	0
Ti (32)	1.01	0.07	N (32)	0	0

Table 5
Charge partitioning for gas molecules – doped graphene by Hirshfeld method.

	C1	C2	C3	Ti or *N*	*N*	*O*	*O*
Ti-doped/NO_2	−0.13	−0.11	0.43	−0.13	0.09	−0.19	−0.14
Ti-doped/NO	−0.12	−0.12	−0.1	0.4	−0.08	−0.05	/
Ti-doped/O_2	−0.08	−0.12	−0.12	0.42	/	−0.19	−0.17
N-doped/NO_2	0.06	0.06	0.06	0.04	0.06	−0.2	−0.2
N-doped/NO	0.05	0.05	0.05	−0.0004	−0.01	−0.02	
N-doped/O_2	0.05	0.05	0.05	0.04		−0.13	−0.13

energy (E_{ads}) of NO_2 and doped graphene, where it is evident that doping the Ti atom could greatly improve the E_{ads}. The E_{ads} is located around −3 eV for Ti-doped graphenes (32, 72, and 200 atoms in total), but improved to about 0.7 eV for the Ti-doped graphene (98 atoms in total). A very special phenomenon could be found in the HOMO–LUMO gap of these systems. The HOMO–LUMO gap of Ti-doped graphene decreased to 0 eV (32, 72, and 200 atoms in total) after the NO_2 adsorption process. However, the HOMO–LUMO gap of Ti-doped graphene (98 atoms in total) basically retained the same value (0.87 eV before and 0.91 eV after) after the NO_2 adsorption process. For the N-doped graphenes, the E_{ads} between NO_2 and N-doped graphene were all very small; in other words, the interactions between NO_2 and N-doped graphene were very weak. The E_{ads} was in the range of –0.5–0.5 eV for all the N-doped graphenes (200, 98, 72, and 32 atoms in total, see Table 2). The HOMO–LUMO gap of N-doped graphene improved with the increase of the graphene size after NO_2 adsorption except for the N-doped graphene with 72 atoms in total. Considering Eq. (2), the recovery time for the NO_2 adsorption process were related directly to the adsorption energy. While the Eq. (3) indicated that the electrical conductivity of the substrate was related with the HOMO–LUMO gap. Thus, N-doped graphene might have a shorter recovery time for NO_2 adsorption than Ti-doped graphene. However, it can be observed that NO_2 adsorption could be used to modulate the HOMO–LUMO gap of Ti- or N-doped graphene. The interactions between NO_2 and Ti- or N-doped graphene had no direct relationship to graphene size.

3.3. NO adsorption on Ti- or N-doped graphene

NO has also attracted considerable interest as a by-product of the combustion of substances in the air. Here we also calculated the interactions between NO and Ti- or N-doped graphenes to investigate whether the phenomenon for the NO_2-Ti- or N-doped graphene still existed. From Table 1, it was found that the interactions between NO and Ti-doped graphene were larger than those between NO and N-doped graphene. The E_{ads} was about −1.4 eV for Ti-doped graphenes (200, 72, and 32 atoms in total), but about −0.62 eV for Ti-doped graphene with 98 atoms in total. The HOMO–LUMO gap variation of Ti-doped graphenes (200, 162, 98, 72, and 32 atoms in total) exhibited the same trends a those found for NO_2-Ti-doped graphenes. There was a difference between the NO_2 and NO adsorption processes. The E_{ads} was the largest for NO_2-Ti-doped graphene (98 atoms in total) and it was the least for NO-Ti-doped graphene (98 atoms in total) (see Table 1).

For N-doped graphenes, the E_{ads}s were located in the range of −0.08 eV to 0.16 eV, which was very similar to those of the NO_2-N-

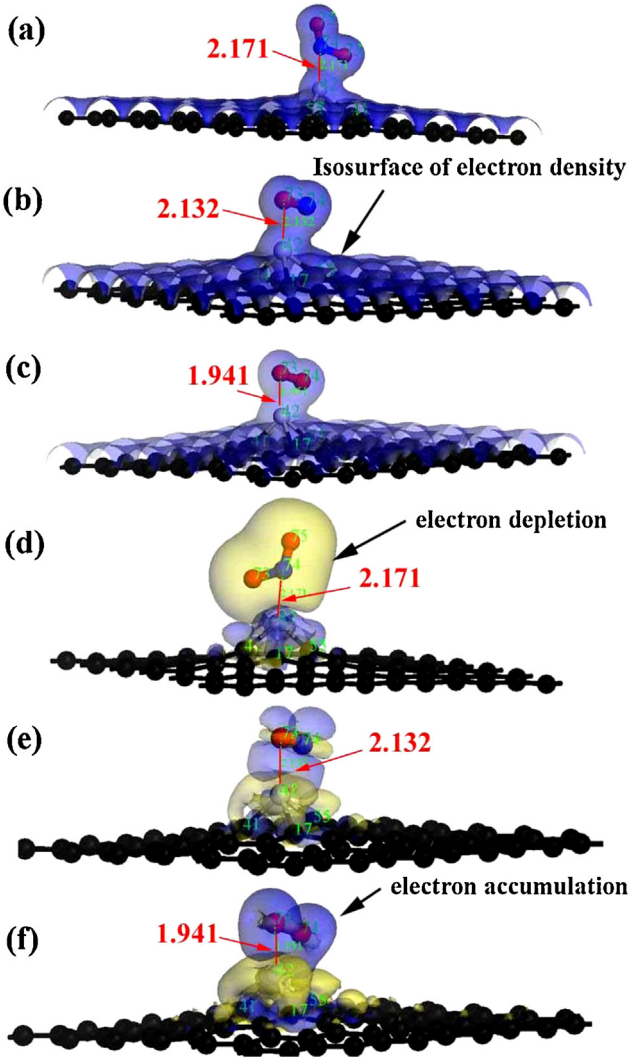

Fig. 5. Isosurface of electron density and electrodensity differences (72 atoms in total): (a) electron density of NO_2-Ti-doped graphene, (b) electron density of NO-Ti-doped graphene, (c) electron density of O_2-Ti-doped graphene, (d) electron density difference of NO_2-Ti doped graphene, (e) electron density difference of NO-Ti-doped graphene, (f) (d) electron density difference of O_2-Ti doped graphene.

doped graphenes. The HOMO–LUMO gap of the N-doped graphene was not changed by NO adsorption. Thus, by comparing the E_{ads} and the HOMO–LUMO gap of the NO-N-doped graphenes and the NO_2-N-doped graphenes, it was concluded that NO did not disturb the detection of the NO_2 with Ti- or N-doped graphene.

3.4. O_2 adsorption on Ti- or N-doped graphene

O_2 was also considered in the simulation systems as a common substance. The E_{ads} between O_2 and Ti-doped graphenes was about −3.4 eV with 32, 72 and 200 atoms in total. But it was about −2.6 eV for the Ti-doped graphene with 98 atoms in total. The HOMO–LUMO gaps of Ti-doped graphenes all clearly decreased after the O_2 adsorption process. For the N-doped graphene, the E_{ads} located in the range of −0.2 eV–0.4 eV. The HOMO–LUMO gap increased a little for the N-doped graphenes with 98 and 200 atoms in total (see Tables 1 and 3). Thus, O_2 adsorption on Ti-doped graphene would also not interfere with detection of the NO_2 molecule. Fig. 5 shows the results of the total electron density and electron density difference analysis. From Fig. 5(a)–(c), it is evident that there were electron interactions between gas molecules and Ti-doped graphene. Fig. 5(d)–(f) show details of the electron accumulation and depletion during the gas adsorption on Ti-doped graphene. On the other hand, the adsorption of gases (NO_2, NO, and O_2) on Ti- or N-doped graphene could be used to modulate the HOMO–LUMO gap of tailored graphenes. These results have not been reported Table 4 elsewhere.

4. Conclusion

The adsorption mechanism of the toxic NO_2 on material surfaces must be elucidated in order to develop new methods for the detection and removal of highly hazardous chemicals in various environments. In this study, DFT calculations were performed to investigate the adsorption of NO_2 molecules onto Ti-, and N-doped graphene sheets. Different sizes of the doped graphenes were considered. The adsorption energy and HOMO–LUMO gaps were carefully calculated and investigated. The results showed that Ti-doped graphene could be used as a NO_2 sensor without considering the effects of the NO and O_2. An interesting phenomenon was found, that doped Ti atoms could modulate the HOMO–LUMO gap of the graphenes and the gas adsorption could also affect the HOMO–LUMO gap of graphenes. This study serves as a basis for the effective design of sensors for environmental remediation.

Acknowledgement

This research was supported by the NSFC (Grant No. 31300793), the Program for New Century Excellent Talents in University (Grant No. NCET-10-0704), and the Engineering Research Center of Biomass Materials (SWUST), Ministry of Education (Grant No. 12zxbk06), China.

References

[1] K.S. Novoselov, A.K. Geim, S.V. Morozov, D. Jiang, Y. Zhang, S.V. Dubonos, I.V. Grigorieva, A.A. Firsov, Electric field effect in atomically thin carbon films, Science 306 (2004) 666–669.
[2] K.S. Novoselov, A.K. Geim, S.V. Morozov, D. Jiang, M.I. Katsnelson, I.V. Grigorieva, S.V. Dubonos, A.A. Firsov, Two-dimensional gas of massless Dirac fermions in graphene, Nature 438 (2005) 197–200.
[3] G. Wang, J. Yang, J. Park, X. Gou, B. Wang, H. Liu, J. Yao, Facile synthesis and characterization of graphene nanosheets, J. Phys. Chem. C 112 (2008) 8192–8195.
[4] S.J. Park, Aqueous suspension and characterization of chemically modified graphene sheets, Chem. Mater. 20 (2008) 6592–6594.
[5] W. Yuan, G. Shi, Graphene-based gas sensors, J. Mater. Chem. A 1 (2013) 10078–10091.
[6] Y. Shao, J. Wang, H. Wu, J. Liu, I.A. Aksay, Y. Lin, Graphene based electrochemical sensors and biosensors: a review, Electroanalysis 22 (2010) 1027–1036.
[7] Y. Chen, X. Yang, Y. Liu, J. Zhao, Q. Cai, X. Wang, Can Si-doped graphene activate or dissociate O_2 molecule? J. Mol. Graphics Modell. 39 (2013) 126–132.
[8] S. Sharma, A.S. Verma, A theoretical study of H_2S adsorption on graphene doped with B, Al and Ga, Physica B 427 (2013) 12–16.
[9] Y.H. Zhang, L.F. Han, Y.H. Xiao, D.Z. Jia, Z.H. Guo, F. Li, Understanding dopant and defect effect on H2S sensing performances of graphene: a first-principles study, Comput. Mater. Sci. 69 (2013) 222–228.
[10] M.I. Rojas, E.P.M. Leive, Density functional theory study of a graphene sheet modified with titanium in contact with different adsorbates, Phys. Rev. B 10 (2007) 1554–15568.
[11] S.B. Chu, L. Hu, X. Hu, M. Yang, J. Deng, Titanium-embedded graphene as high-capacity hydrogen-storage media, Int. J. Hydrogen Energy 36 (2011) 12324–12328.
[12] H.P. Zhang, X.G. Luo, X.Y. Lin, X. Lu, Y. Leng, H.T. Song, Density functional theory calculations on the adsorption of formaldehyde and other harmful gases on pure, Ti-doped, or N-doped graphene sheets, Appl. Surf. Sci. 283 (2013) 559–565.
[13] Z.M. Ao, F.M. Peeters, High-capacity hydrogen storage in Al-adsorbed graphene, Phys. Rev. B 81 (2011) 2054–2059.
[14] S.W. Choi, A. Katoch, G.J. Sun, S.S. Kim, Bimetallic Pd/Pt nanoparticle-functionalized SnO_2 nanowires for fast response and recovery to NO_2, Sens. Actuators B: Chem. 181 (2013) 446–453.
[15] C.Y. Lin, W.T. Huang, C.T. Wu, K.C. Ho, Electrochemical reduction of NO_2 at a Pt/membrane electrode-Application to amperometric NO_2 sensing, Sens. Actuators B: Chem. 136 (1) (2009) 32–38.
[16] M. Rivallan, G. Ricchiardi, S. Bordiga, A. Zecchina, Adsorption and reactivity of nitrogen oxides (NO_2, NO, N_2O) on Fe-zeolites, J. Catal. 26 (2009) 104–116.
[17] E.C. Anota, A.T. Soto, G.H. Cocoletzi, Studies of graphene - chitosan interactions and analysis of the bioadsorption of glucose and cholesterol, Appl. Nanosci. 4 (2014) 911–918.
[18] T. Samerjai, N. Tamaekong, C. Liewhiran, A. Wisitsoraat, S. Phanichphant, NO_2 gas sensing of flame-made Pt-loaded WO_3 thick films, J. Solid State Chem. 214 (2014) 47–52.
[19] J. Zhao, T. Yang, Y. Liu, Z. Wang, X. Li, Y. Sun, Y. Du, Y. Li, G. Lu, Enhancement of NO_2 gas sensing response based on ordered mesoporous Fe-doped In_2O_3, Sens. Actuators B: Chem. 191 (2014) 806–812.
[20] J. Esmaeilzadeh, S. Ghashghale, P.S. Khianbani, A. Hosseinmardi, E. Marzbanrad, B. Raissi, C. Zamani, Effect of dispersant on chain formation capability of TiO_2 nanoparticles under low frequency electric fields for NO_2 gas sensing applications, J. Eur. Ceram. Soc. 34 (2014) 1201–1208.
[21] B. Saruhan, A. Yuce, Y. Gonullu, K. Kelm, Effect of Al doping on NO_2 gas sensing of TiO_2 at elevated temperatures, Sens. Actuators B: Chem. 187 (2013) 586–597.
[22] R. Pearce, T.I.M. Andersson, L. Hultman, A.L. Spetz, R. Yakimova, Epitaxially grown graphene based gas sensors for ultra sensitive NO_2 detection, Sens. Actuators B: Chem. 155 (2011) 451–455.
[23] B. Delley, From molecules to solids with the $DMol^3$ approach, J. Chem. Phys. 113 (2000) 7756–7764.
[24] G.A. Petersson, M.A. Al-Laham, A complete basis set model chemistry. II. Open-shell systems and the total energies of the first-row atoms, J. Chem. Phys. 94 (1991) 6081–6090.
[25] G.A. Petersson, A. Bennett, T.G. Tensfeldt, M.A. Al-Laham, W.A. Shirley, J. Mantzaris, A complete basis set model chemistry. I. The total energies of closed-shell atoms and hydrides of the first-row atoms, J. Chem. Phys. 89 (1988) 2193–2218.
[26] B. Delley, An all-electron numerical method for solving the local density functional for polyatomic molecules, J. Chem. Phys. 92 (1990) 508–517.
[27] B. Delley, Hardness conserving semilocal pseudopotentials, Phys. Rev. B 66 (2002) 155125.
[28] J.P. Perdew, K. Burke, M. Ernzerhof, Generalized gradient approximation made simple, Phys. Rev. B 77 (1996) 3865–3868.
[29] M.K.Y. Chan, G. Ceder, Efficient band gap prediction for solids, Phys. Rev. Lett. 105 (2010) 196403–196404.
[30] H.J. Monkhorst, J.D. Pack, Special points for Brillouin-zone integrations, Phys. Rev. B 13 (1976) 5188–5192.
[31] B.R. Matis, J.S. Burgess, F.A. Bulat, A.L. Friedman, B.H. Houston, J.W. Baldwin, Surface doping and HOMO–LUMO gap tunability in hydrogenated graphene, ACS Nano 6 (2012) 17–22.
[32] L.A. Chernozatonskii, Similarity in HOMO–LUMO gap behavior of modified graphene with different types of functionalization, J. Phys. Chem. C 118 (2014) 1318–1321.